remote sensing

MDPI

Article

Asian Rice Calendar Dynamics Detected by Remote Sensing and Their Climate Drivers

Jing Zhang [1,2,3], Huaqing Wu [1,2,4], Zhao Zhang [1,2,4,*], Liangliang Zhang [1,2,4], Yuchuan Luo [1,2,4], Jichong Han [1,2,4] and Fulu Tao [5,6,7]

1 State Key Laboratory of Earth Surface Processes and Resource Ecology (ESPRE), Beijing Normal University, Beijing 100875, China
2 Academy of Disaster Reduction and Emergency Management, Ministry of Emergency Management and Ministry of Education, Beijing 100875, China
3 Faculty of Geographical Science, Beijing Normal University, Beijing 100875, China
4 School of National Safety and Emergency Management, Beijing Normal University, Beijing 100875, China
5 Key Laboratory of Land Surface Pattern and Simulation, Institute of Geographical Sciences and Natural Resources Research, Chinese Academy of Sciences, Beijing 100101, China
6 College of Resources and Environment, University of Chinese Academy of Sciences, Beijing 100049, China
7 Natural Resources Institute Finland (Luke), FI-00790 Helsinki, Finland
* Correspondence: zhangzhao@bnu.edu.cn

Abstract: Detecting crop calendar changes is critically important for crop monitoring and management, but the lack of annual, Asia-wide, and long-term rice calendar datasets limits our understanding of rice phenological changes and their climate drivers. In this study, we retrieved key rice phenological dates from the GLASS AVHRR LAI through combining threshold-based and inflection-based detection methods, analyzed the changes during the period 1995–2015, and identified the key climate drivers of the main rice seasons in Asia. The retrieved phenological dates had a high level of agreement with the referenced observations. All R^2 were greater than 0.80. The length of the vegetation growing period (VGP) was mostly shortened (by an average of −4 days per decade), while the length of the reproductive growing period was mostly prolonged (by an average of 2 days per decade). Moreover, solar radiation had the most significant impact on the rice calendar changes, followed by the maximum and minimum temperatures. The VGP in tropical areas is the most sensitive to climate change. Our study extends the annual rice phenology dynamics to a higher spatial–temporal resolution and provides new insights into rice calendar changes and their climate drivers, which will assist governments and researchers regarding food security and agricultural sustainability.

Keywords: remote sensing; crop phenology; paddy rice; calendar changes; climate contribution; Asia

Citation: Zhang, J.; Wu, H.; Zhang, Z.; Zhang, L.; Luo, Y.; Han, J.; Tao, F. Asian Rice Calendar Dynamics Detected by Remote Sensing and Their Climate Drivers. *Remote Sens.* **2022**, *14*, 4189. https://doi.org/10.3390/rs14174189

Academic Editors: Luo Liu, Yuanwei Qin, Bingwen Qiu, Qiangyi Yu and Zhi Qiao

Received: 14 July 2022
Accepted: 22 August 2022
Published: 25 August 2022

1. Introduction

A crop calendar consists of the key phenological stages in the crop's growth cycle, such as transplanting, heading, and harvesting dates for rice. The biophysical and biochemical features of plants vary significantly in different phenological stages, and thus changes of the crop calendar are critically important for agricultural monitoring systems [1,2]. Paddy rice is the most important staple crop grown by smallholder farmers in Asia. Many studies have shown various changes in the timing of major phenological event for rice in specific Asian countries, such as the earlier heading date in Japan [3] and delayed heading date in China [4]. Such complicated and highly heterogeneous phenology changes affect the ecosystem structure, crop productions, and their climatic feedbacks [1,2]. Therefore, knowing how and why the rice calendar is changing will help farmers improve their field management and sustain their livelihoods under climate change [5,6]. The first rice calendar dates back thousands of years, but today, continuous crop calendars are spatially scarce and temporally short-termed [7]. For example, the United States Department of Agriculture (USDA) provides monthly rice calendar windows at the national scale without indicating

specific phenological dates in different years (https://ipad.fas.usda.gov/Default.aspx, accessed on 11 August 2022), and the RiceAtlas [6] collects planting and harvesting dates at 1121 administrative units across 31 countries in Asia but ignores annual changes over time. Therefore, our understandings of rice calendar changes are so far limited.

In recent decades, sophisticated monitoring technologies and modelling approaches started the modern phenology ear [1]. In particular, a time series of spectral vegetation indexes, for example, the leaf area index (LAI), can capture dynamic vegetation characteristics at key phenological stages [1,8,9]. Therefore, the rapid development of remote sensing has significantly expanded the scope of phenology studies across large areas [1,10,11]. More crop calendar datasets are now being generated and made publicly available, such as PhenoRice [12], ChinaCropPhen1km [13], and RICA [7]. However, because of different research goals and technological constraints, these rice calendar datasets only focus on a particular country (e.g., ChinaCropPhen1km focuses on China), limited phenological dates (e.g., RICA focuses on start and end of season), or a short period (e.g., PhenoRice focuses on the period 2012–2014). Thus, a long-term, Asia-wide rice calendar remains unavailable.

Climate change has a significant impact on crop calendars [14,15]. The response of phenology to climate is nonlinear [16] and provides concomitant feedbacks to multiple ecological processes. Regarding rice, previous studies using statistics or remote sensing data have identified some regional characteristics in terms of calendar changes and how temperature has influenced rice calendars as a result of global warming. For example, as a result of the decreased temperature during the booting stage, the rice heading date in Japan became 0.7–1.9 days earlier per decade during 1961–2010 [3]. Luo et al. [13] found that the rice growing period in China was prolonged by 0–2 days per year from 2000 to 2015, based on phenological dates retrieved from the Global LAnd Surface Satellite (GLASS) LAI. However, we know little about the impacts of other climate variables, such as wind speed and solar radiation. In addition, these studies do not provide a comprehensive understanding of rice calendar changes across the whole of Asia because their studied periods and areas differed greatly. Therefore, we aim to provide a comprehensive understanding of the drivers and mechanisms underlying rice calendar changes using long-term rice calendars retrieved from remote sensing data.

Along this line, the study objectives in relation to main rice-cropping seasons in Asia are as follows: (1) identify the long-term phenological dates (transplanting, heading, and harvesting dates) based on remote sensing; (2) investigate dynamic changes of the rice calendar; and (3) specify the key climate drivers of those changes.

2. Materials and Methods

2.1. Study Area

Rice cropping systems are diverse and complicated in Asia, where rice is often cultivated multiple times or in a rotation with other crops each year [6,12,13]. To identify the most continuous and important rice calendar characteristics, we used the definitions of rice season from the USDA and RiceAtlas and focused on 17 main cropping seasons in 14 countries in Asia (Figure 1 and Table 1). Notably, China, India, and Vietnam have two main cropping seasons with various growing periods (Table 1) in different areas (Figure 1). To specify such two different main cropping seasons, we also used "2ed" main season to represent the late season in China, Kharif season in India, and winter season in Vietnam in Figure 1 and Table 1. Generally, monthly rice seasons range from April to December, and with some exceptions to the March of the next year (Table 1). Based on the annual dataset of the paddy rice area at 500 m resolution (APRA500) [17], the rice-cropping area in Figure 1 is the maximum paddy rice area, where rice grows for at least one year.

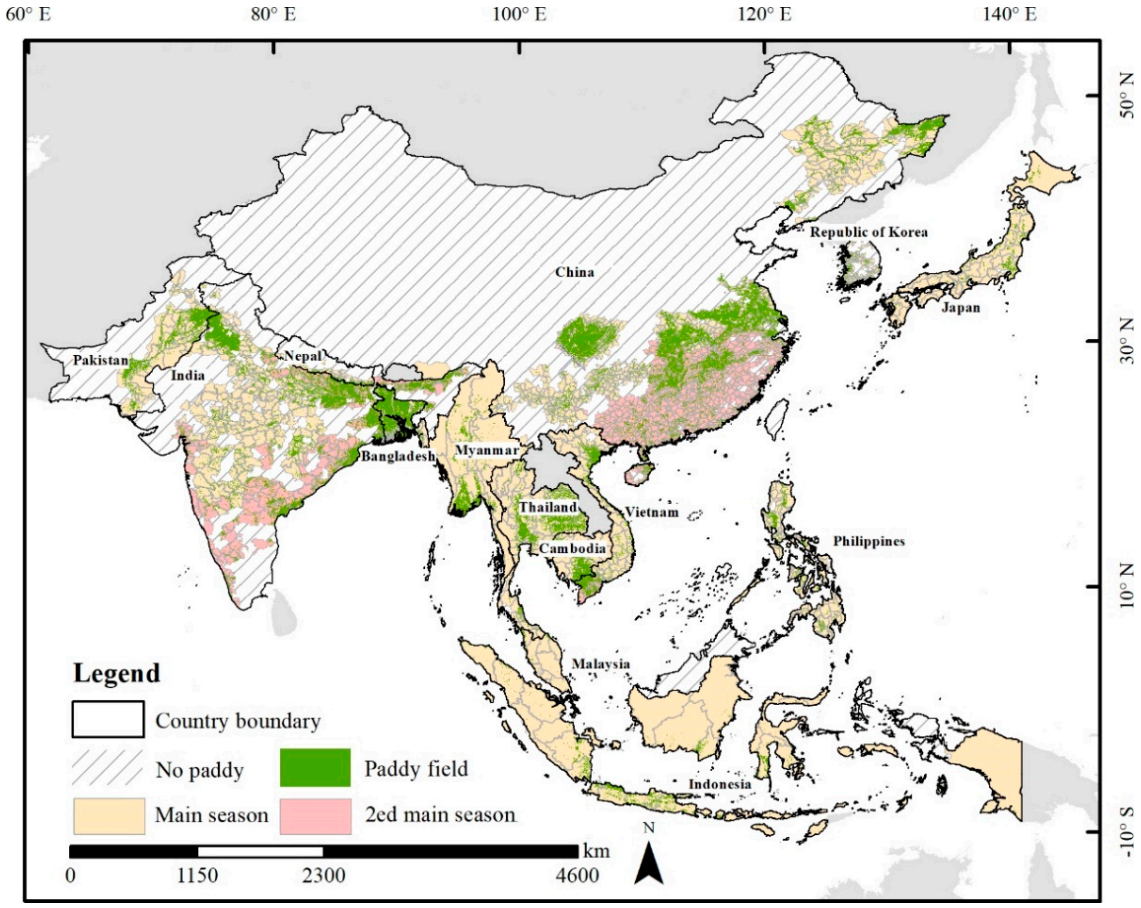

Figure 1. Main rice-cropping seasons and areas in Asia. Country map comes from the National Standard Map Service (http://bzdt.ch.mnr.gov.cn/, accessed on 11 August 2022). Paddy fields represent the maximum paddy rice area where paddy rice grows for at least one year based on an annual dataset of paddy rice area at 500 m resolution (APRA500) [17].

Table 1. Main rice-cropping seasons in Asia.

Country	Local Name of the Main Season	Administrative Unit [1]	Crop Calendar
Bangladesh	Aman	District	May–December
Cambodia	Wet	Province	June–February
Indonesia	Main	Province	August–March
Japan	Single	Prefectural	April–October
Malaysia	Main	State	September–February
Myanmar	Single	State	June–November
Nepal	Single	District	May–December
Pakistan	Single	District	May–December
Philippines	Main	Province	April–December
Republic of Korea	Single	Town	May–October
Thailand	Wet	Province	May–December
China	Single Late (2ed)	County	April–September July–November
India	Single Kharif (2ed)	District	May–November June–January
Vietnam	Autumn Winter (2ed)	Province	June–November November–March

[1] The "Administrative Unit" is the spatial unit with available ground rice calendars at a subnational level for each country.

2.2. Data

2.2.1. Ground Rice Calendars

In this study, we used ground rice calendars from the USDA (https://ipad.fas.usda.gov/Default.aspx, accessed on 11 August 2022), RiceAtlas [6] and census-based observations from previous studies and agrometeorological stations [3,4]. The USDA identifies the main cropping seasons and the monthly growing stages at the country scale, and the RiceAtlas provides more subnational public calendar data for the start, peak, and end of the sowing/transplanting and harvesting periods. Although the USDA and RiceAtlas are both not annually dynamic, they provide ranges of various growing stages and thereby can validate remote-sensing-retrieved phenological dates (see Section 2.3). In addition, census-based observations offer some seasonal rice calendar information that provides further validation of remote-sensing-retrieved phenological dates. For example, the observed rice calendars from hundreds of Chinese agrometeorological stations include detailed phenological dates for main rice seasons since 1981 [4].

2.2.2. Remote Sensing Data

To obtain the long-term rice calendars, we used the GLASS LAI data from the Advanced Very High-Resolution Radiometer (AVHRR) during the period 1995–2015 (http://glass.umd.edu/Download.html, accessed on 12 July 2022) [18,19]. The GLASS AVHRR LAI is produced by general regression neural networks, with a spatial resolution of 0.05° (~5 km) and a temporal resolution of 8 days. Compared with other similar LAI products (NCEI AVHRR [20], GIMMS3g [21], and GLOBMAP [22]), GLASS AVHRR LAI has the minimum root mean square error (RMSE) and bias (0.90 and −0.19) against LAI values from high-resolution reference maps [23] and has been widely applied in vegetation crop studies [24–26].

2.2.3. Climate Variables

TerraClimate [27] data were used to evaluate how climatic variables impact rice calendar changes in this study. To conduct a comprehensive analysis, we selected six climatic variables, including the monthly maximum temperature (t_{max}), minimum temperature (t_{min}), precipitation (*ppt*), downward surface shortwave radiation (*srad*), vapor pressure (*vap*), and wind speed (*ws*) at approximately 4 km × 4 km of spatial resolution.

2.3. Methods

2.3.1. Phenological Dates Retrieved from GLASS AVHRR LAI

A rice calendar consists of three key phenological dates: transplanting, heading, and harvesting dates, which divide the whole growing period (GP) into the vegetation growing period (VGP) and the reproduction growing period (RGP). Using the GLASS AVHRR LAI, we generated phenological dates following the steps shown in Figure 2:

(1) We determined the pure grids for the main rice-cropping seasons based on the threshold method. First, we resampled paddy rice grids from the original resolution of APRA500 (500 m) to the resolution of the GLASS AVHRR LAI (0.05°) so that we could assign GLASS AVHRR LAI values to each 0.05° × 0.05° paddy rice grid. However, grids with the rice-specific LAI time series vary greatly among different rice seasons in each year because of the mixed-pixel problems and cloud pollution of remote sensing data. Therefore, second, we used the monthly growing windows information from the USDA (Table 1) as the thresholds to extract the LAI time series for each rice season at grid scale. For example, only LAI values during the period May–Dec were used for rice in Bangladesh. RiceAtlas [6] provided the start and end dates of the transplanting, heading, and harvesting periods, and we further applied them to each grid. Finally, the grid would be filtered out if half of its LAI time series was beyond the long-term average ± two times the standard deviation during 1995–2015. The rest of the grids were so-called "pure grids," the LAI time series of which could reflect dynamic vegetation characteristics at key phenological stages of rice.

(2) We retrieved the transplanting, heading, and harvesting dates from the LAI curve, based on the inflection-based method. Generally, the LAI remains at a low value before transplanting and then rapidly increases after this date. Therefore, if the first derivative is greater than 0 or the second derivative is equal to 0 at one point on the LAI curve during the transplanting period, this point indicates the transplanting date [28,29]. The heading date is at the inflection point with the peak LAI value on one LAI curve [30]. Finally, the point on the LAI curve has a negative first derivative value at the harvesting date because crop activities drop sharply during the harvesting period [9]. Furthermore, if there were imperfect LAI time series at grid scale, we also considered other remote-sensing-retrieved rice calendars in an effort to improve our results, for example, ChinaCropPhen1km [13].

(3) We aggregated phenological dates from grids into administrative units (see Table 1) and assessed their accuracy assessment by comparing them with the ground rice calendars (see Section 2.2.1). In addition, the average of the retrieved phenological dates during 1995–2015 was calculated at the administrative unit scale to enable us to compare their accuracy with the peak value of each growing stage published in the RiceAtlas. Considering that the RiceAtlas had no heading date information, we used the midpoint of mid-season from the USDA as the referenced heading date for the accuracy assessment. The seasonally phenological dates from census-based observations also provided reference data for the accuracy assessment. The coefficient of determination (R^2) and RMSE were used to evaluate the accuracy of the retrieved phenological dates for each rice season as follows:

$$R^2 = 1 - \frac{\sum_{i=1}^{n} (\text{Pheno}_{\text{rs},\,i} - \text{Pheno}_{\text{obs},\,i})^2}{\sum_{i=1}^{n} (\text{Pheno}_{\text{obs},\,i} - \overline{\text{Pheno}_{\text{obs}}})^2} \quad (1)$$

$$\text{RMSE} = \sqrt{\frac{\sum_{i=1}^{n} (\text{Pheno}_{\text{rs},\,i} - \text{Pheno}_{\text{obs},\,i})^2}{n}} \quad (2)$$

where n is the number of administrative units and $i = 1, 2, \ldots, n$. $\text{Pheno}_{\text{obs},\,i}$ represents the observed phenological dates from the USDA, RiceAtlas, and census-based observations at the ith administrative unit. $\overline{\text{Pheno}_{\text{obs}}}$ is the average phenological date across all administrative units. $\text{Pheno}_{\text{rs},\,i}$ represents the phenological date retrieved from remote sensing data at the ith administrative unit.

2.3.2. Sensitivity Analysis

To evaluate the impacts of climate change on rice calendars, we calculated the sensitivity of different growing stages to climate variables using Equation (3), according to Liu et al. [31]:

$$\Delta\text{Period} = \text{S1} \times \Delta\sum t_{max} + \text{S2} \times \Delta\sum t_{\min} + \text{S3} \times \Delta\sum ppt + \text{S4} \times \Delta\sum srad + \text{S5} \times \Delta\sum vap + \text{S6} \times \Delta\sum ws + \text{b} \quad (3)$$

where Δ represents the difference between the next year and the current year, so that we can avoid the effect of time trends. The Period in Equation (3) can be the VGP, RGP, and GP. The sum ($\sum$) of each climate variable is calculated during the Period. The corresponding S represents the slope of the equation (the so-called sensitivity factor), indicating the impact of each weather variable to the Period, and b represents the intercept of the regression model. All variables in Equation (3) have been standardized into [–1,1]. Nevertheless, only the "Δclimate variable" that was partially correlated with "ΔPeriod" at the 0.05 significance level could be included in Equation (3) for each administrative unit.

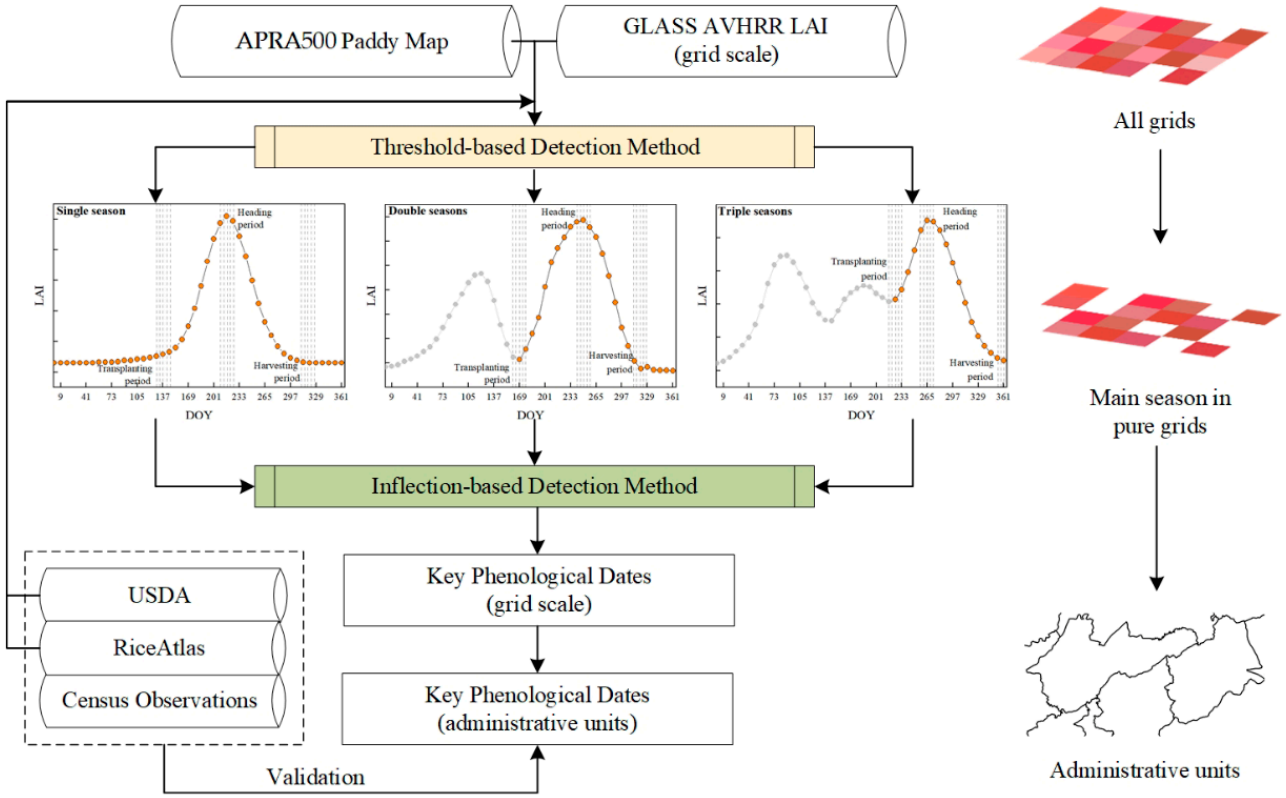

Figure 2. The workflow for retrieving key phenological dates from the GLASS AVHRR LAI.

3. Results

3.1. Accuracy Assessment of the Remote-Sensing-Retrieved Phenological Dates

The comparison between the retrieved phenological dates and the observations were closely around the 1:1 line in Figure 3. In general, the RMSE was 9 days, 13 days, and 14 days for the transplanting, heading, and harvesting date, respectively, with the corresponding R^2 of 0.91, 0.83, and 0.96, respectively. The lowest R^2 (0.83) might have resulted from the underestimations of the retrieved heading dates (Figure 3b). The increase in RMSE from the transplanting date via the heading date to the harvesting date (9 < 13 < 14 days) indicated that errors in retrieving phenological dates tended to be cumulative. Although the error of some outliers was >16 days, the proportion of error $\leq$ 16 days was as high as 90%, 85%, and 75% for the transplanting, heading, and harvesting date, respectively (Figure 3).

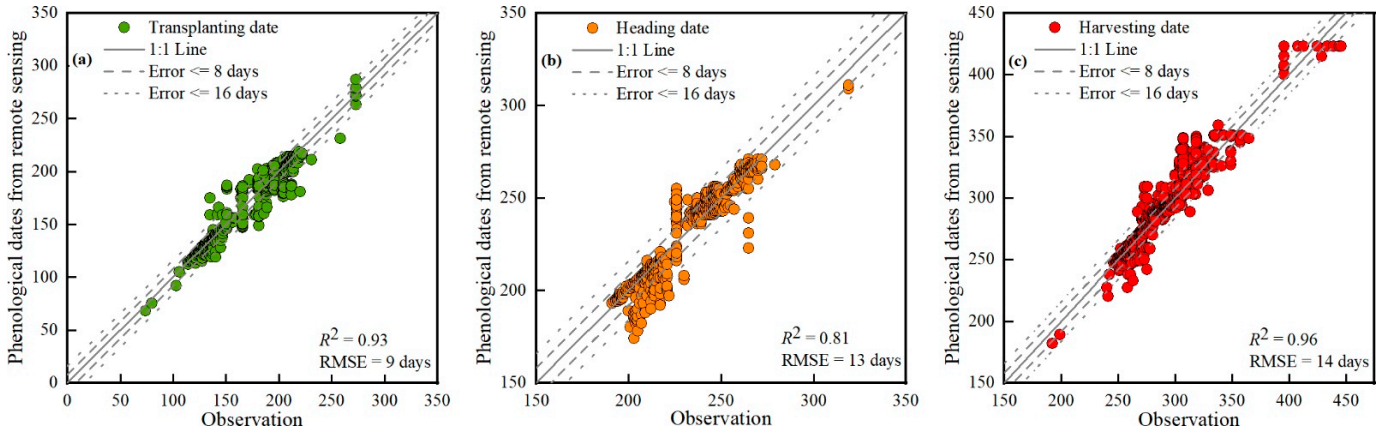

Figure 3. The 1:1 comparison between the retrieved phenological dates and observations at the administrative scale for (**a**) transplanting date, (**b**) heading date, and (**c**) harvesting date.

Figure 4 showed the average length of different growing stages across the whole study area, based on the retrieved phenological dates. The VGP and RGP ranged from 30 to 120 days, except for a longer period (120 to 150 days) in Indonesia and the Philippines (Figure 4a,b). As for the differences between VGP and RGP, the length of the latter was somehow longer than the former at the grids for rice seasons in China, Thailand, and the Philippines because of the underestimations of heading dates. The GP was mainly in a range from 120 to 180 days, but some grids had a shorter period (<120 days) for Aman season in Bangladesh, the late season in China, and winter season in Vietnam, while some grids had a longer period (>180 days) for rice seasons in the Republic of Korea, Japan, Indonesia, and Philippines (Figure 4c). Specifically, grids with the shortest GP length were mainly distributed in late-season areas in China and winter-season areas in Vietnam, where multiple crops were grown each year.

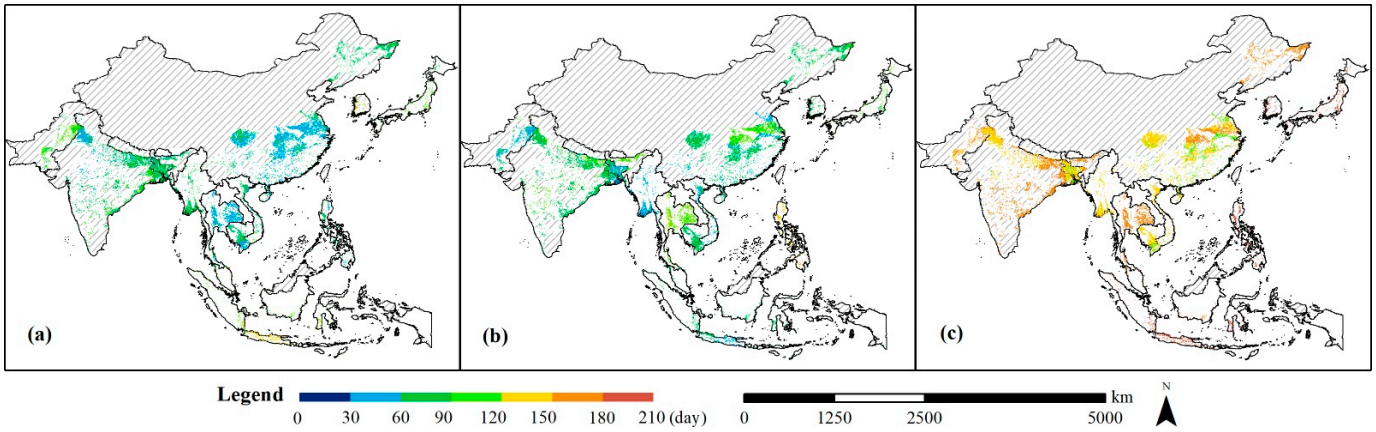

Figure 4. The average length of the growing seasons during 1995–2015 at grid scale for: (**a**) VGP, (**b**) RGP, and (**c**) GP.

3.2. Dynamic Changes of Rice Calendars in Asia

Through regressing the length of the growing period and time, we found that during the period 1995–2015, the length of the growing stage significantly changed at 22%, 34%, and 24% of all administrative units for the VGP, RGP, and GP at the significance level of 0.05, respectively (Figure 5(a-1–c-1)). Administrative units with significant changes had distinct spatial-clustering characteristics. For example, all growing stages were prolonged at most administrative units for the late rice season in China. In Myanmar, most administrative units had a greater decrease in the VGP length (average: −4 days per decade, Figure 5(a-1) than the increase of RGP length (average: 2 days per decade, Figure 5(b-1)); therefore, the GP was shortened by around 2 days per decade (Figure 5(c-1)).

Statistically, the average length of the VGP shortened in 12 rice-cropping seasons, except for that in Indonesia, Malaysia, China (single season), India (single season), and Vietnam (autumn season) (Figure 5(a-2)). On the contrary, the average length of the RGP was prolonged in 13 rice-cropping seasons, except for Indonesia, Malaysia, India (single season), and Vietnam (winter season) (Figure 5(b-2)). As a result, the average length changes of the GP varied greatly across all of Asia (Figure 5(c-2)), where rice-cropping seasons were prolonged by at least 2 days in four countries (Indonesia, Japan, Nepal, and China (late season)), shortened by at least 1 day in five countries (Cambodia, Myanmar, Pakistan, the Republic of Korea, and India (single season)), and period changes of the rest of the rice-cropping seasons were close to 0. In addition, the greatest changes were the average of −16 days per decade for the VGP (Figure 5(a-2)) and 13 days per decade for the RGP (Figure 5(b-2)) in the Republic of Korea, while the greatest average change in GP (Figure 5(c-2)) was 10 days per decade in Nepal.

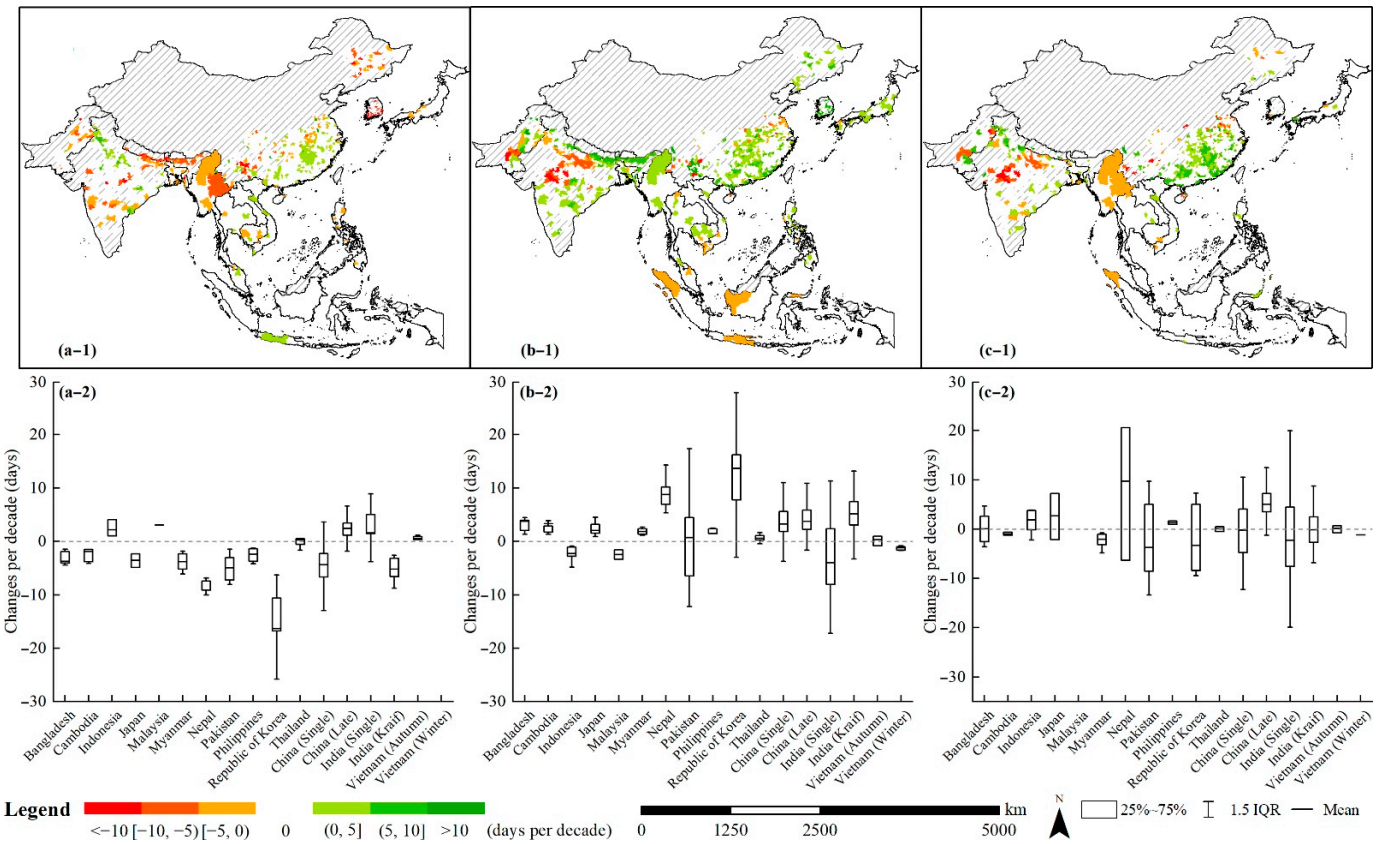

Figure 5. Rice calendar changes per decade for: (**a**) VGP, (**b**) RGP, and (**c**) GP.

3.3. Impacts of Climate Variables on Rice Calendars

To investigate how climate change affected rice calendars, we regressed climate variables and the length of growing stages according to Equation (3) at the administrative unit scale and then aggregated the sensitivity factors to country level in Figure 6. All regressions were significant at the 0.05 level.

In general, *srad*, t_{max}, t_{min}, and *vap* were the climate variables that had the greatest impacts on rice calendars. Specifically, *srad* had the greatest positive impacts in almost all seasons, with the average sensitivity factor of 0.51, 0.69, and 0.71 for the VGP, RGP, and GP, respectively. The effects of t_{max} and t_{min} varied substantially across different periods and seasons. Compared with t_{max}, t_{min} had more negative sensitivity factors during all periods (VGP: 5 > 1; RGP: 9 > 7; GP: 8 > 5), indicating that an increase in t_{min} was more effective in shortening the growing period. As for different growing stages, the VGP was the most vulnerable to temperature changes, with the averaged sensitivity factor of 0.48 for t_{max} and 0.42 for t_{min} (Figure 6a). Regarding RGP and GP, the average values of temperature-related sensitivity factors were around 0, even though they ranged from −1.74 to 3.00 across different rice-cropping countries and seasons. Spatially, the negative effects of *vap* were mainly located at the center of study area, such as Pakistan, Nepal, India, Myanmar, and Vietnam (15°N < latitude < 30°N). The effects of *ws* increased as the latitude decreased, especially in Malaysia and Indonesia. Nevertheless, *ppt* had the weakest effect on the length of growing periods, possibly because the paddy rice was well-irrigated.

In addition, more climate variables had stronger impacts on calendar changes as latitude decreased, as represented by the lower triangular matrixes in Figure 6. For example, in Figure 6c, only the sensitivity factors of *srad* were greater than 0.50 in the first four seasons (central latitude > 30°N), but sensitivity factors of five climate variables were greater than 0.50 (or less than −0.50) in the last four seasons (central latitude < 15°N). Such

phenomenon indicated that rice calendars in the lower-latitude areas had more vulnerable and complicated responses to climate change.

Period	Country (Season)	*srad*	t_{max}	t_{min}	*vap*	*ws*	*ppt*
(a) VGP	Japan (Single)	0.81	0.08	−0.36	0.75	0.19	0.06
	Republic of Korea (Single)	0.93	0.11	−0.11	0.03	0.22	0.15
	China (Single)	0.86	0.35	−0.57	0.03	0.28	0.09
	China (Late)	0.28	0.73	−0.02	−0.17	0.04	0.08
	Pakistan (Single)	0.79	0.78	0.53	−0.18	0.06	0.04
	Nepal (Single)	0.85	0.53	0.94	−0.22	0.41	−0.13
	Bangladesh (Aman)	−0.12	0.49	0.85	−0.29	0.20	0.10
	India (Single)	0.37	1.54	0.59	−0.57	0.22	0.17
	India (Kharif)	0.89	1.08	0.37	−0.74	0.11	0.07
	Myanmar (Single)	−1.24	0.94	2.31	−1.25	0.16	0.04
	Vietnam (Autumn)	0.98	−0.02	−0.10	−0.44	0.08	0.04
	Vietnam (Winter)	−0.04	0.07	0.91	0.26	−0.51	0.12
	Thailand (Wet)	1.25	−0.48	−0.82	0.69	−0.03	0.06
	Cambodia (Wet)	0.95	1.40	1.65	−1.35	0.09	0.02
	Philippines (Main)	1.04	0.29	0.14	−0.48	0.08	0.05
	Malaysia (Main)	0.04	0.19	1.16	0.13	−0.21	0.13
	Indonesia (Main)	0.00	0.01	−0.41	0.88	0.53	0.15
(b) RGP	Japan (Single)	0.77	0.34	−0.30	0.24	0.25	0.02
	Republic of Korea (Single)	0.76	0.97	−1.03	0.61	0.24	0.05
	China (Single)	0.70	0.44	−0.20	−0.02	0.25	0.08
	China (Late)	0.70	0.33	−0.24	−0.01	0.13	0.04
	Pakistan (Single)	0.61	1.21	−0.40	−0.53	0.01	−0.03
	Nepal (Single)	0.84	0.42	1.49	−1.13	−0.07	−0.01
	Bangladesh (Aman)	0.73	−0.84	−0.66	1.35	0.03	0.07
	India (Single)	0.77	0.33	0.15	−0.11	0.07	−0.01
	India (Kharif)	0.73	−0.16	0.39	0.04	0.16	0.03
	Myanmar (Single)	0.59	0.29	0.23	−0.32	0.00	0.15
	Vietnam (Autumn)	0.76	−0.37	0.12	−0.11	0.00	−0.02
	Vietnam (Winter)	−0.04	−1.40	3.00	−0.46	0.04	−0.05
	Thailand (Wet)	1.09	−0.40	−0.74	0.78	−0.01	0.00
	Cambodia (Wet)	1.15	−0.32	−1.74	1.57	−0.04	0.15
	Philippines (Main)	1.43	−0.39	−1.23	0.80	−0.04	0.05
	Malaysia (Main)	0.17	0.93	1.65	0.09	−1.44	−0.13
	Indonesia (Main)	−0.04	0.02	0.84	0.59	−0.55	0.00
(c) GP	Japan (Single)	0.80	0.20	−0.13	0.17	0.10	0.01
	Republic of Korea (Single)	0.69	−0.23	0.17	0.06	0.17	−0.04
	China (Single)	0.65	0.30	−0.27	0.16	0.15	0.06
	China (Late)	0.69	0.48	−0.42	0.01	0.10	0.07
	Pakistan (Single)	0.97	0.52	−0.45	0.44	−0.07	0.03
	Nepal (Single)	0.89	0.71	−0.27	0.01	−0.07	−0.08
	Bangladesh (Aman)	0.58	−0.50	−0.28	0.70	0.04	0.16
	India (Single)	1.10	0.34	0.08	−0.39	0.09	−0.01
	India (Kharif)	0.97	0.11	0.65	−0.50	0.05	0.00
	Myanmar (Single)	0.68	0.27	0.20	−0.16	0.01	0.02
	Vietnam (Autumn)	0.77	−0.03	0.05	−0.04	−0.04	0.01
	Vietnam (Winter)	−0.02	0.00	0.64	0.08	0.04	−0.04
	Thailand (Wet)	0.97	−0.22	−0.94	0.88	0.00	0.00
	Cambodia (Wet)	1.04	−0.24	1.00	−1.03	0.12	−0.02
	Philippines (Main)	1.38	−0.60	−0.46	0.40	−0.07	−0.06
	Malaysia (Main)	−0.09	0.12	0.03	0.49	1.14	0.04
	Indonesia (Main)	0.02	0.00	1.10	−0.08	−0.06	0.01

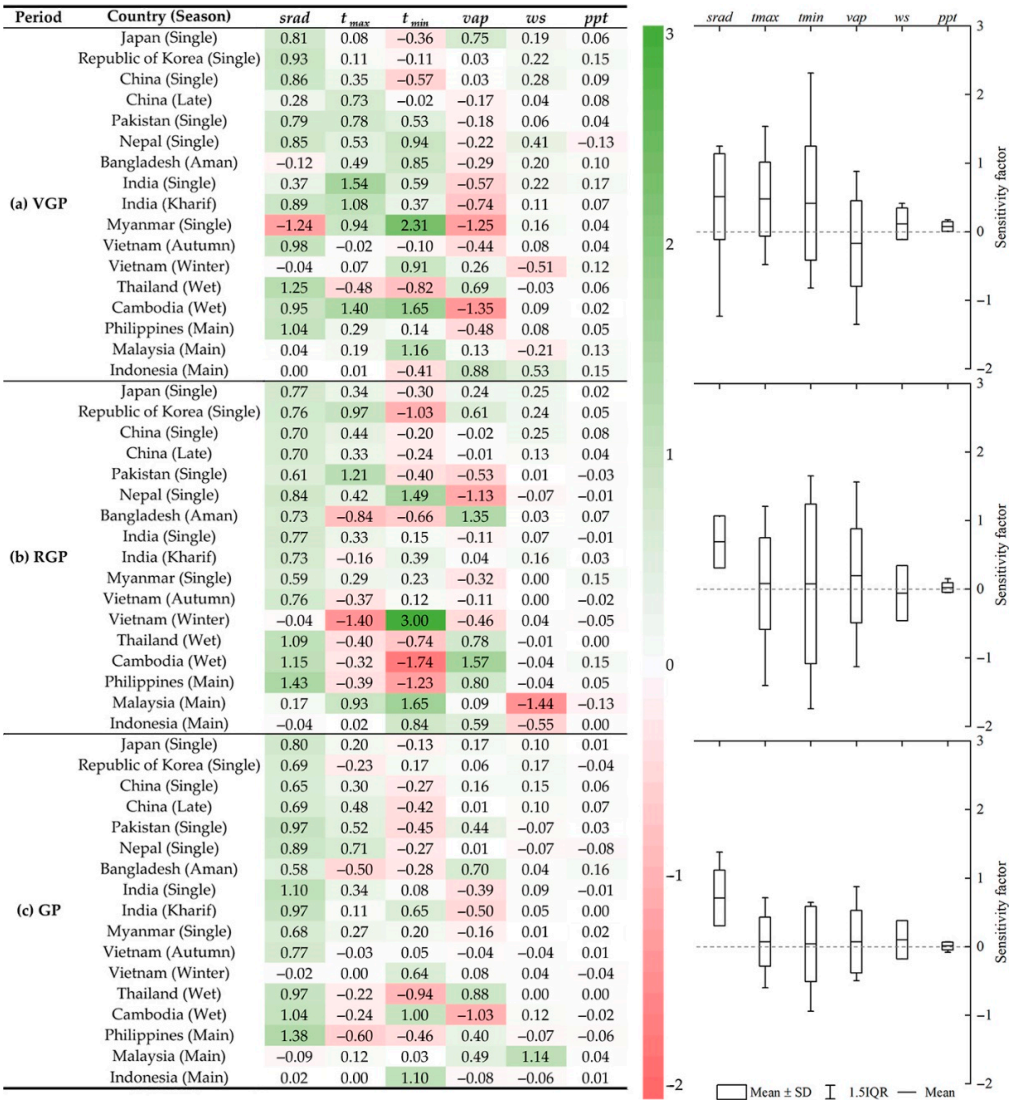

Figure 6. The sensitivity factors of climate variables to rice calendar changes for: (**a**) VGP, (**b**) RGP, and (**c**) GP. Seasons are sorted by the decreasing central latitude. All sensitivity factors were at the 0.05 significance level.

4. Discussion

4.1. An Extended Rice Calendar Based on Remote Sensing in Asia

Based on the LAI time series from the GLASS AVHRR, we retrieved three key phenological dates (transplanting, heading, and harvesting dates) at more than 80,000 grids across 1992 administrative units in 17 main rice-cropping seasons during 1995–2015. Such a large amount of spatiotemporal data provided reliable and critical rice calendar information. Compared with previous studies that focused on either a single country or a short-term period [13,32–34], this study extended crop phenology research from a national scale to a continental scale at a decadal timeline. Considering the adoption of similar crop-growth processes and remote-sensing-produced vegetation indexes around the world, our workflow in Figure 2 could be applied to a wide range of phenological dates, crops, and countries. For example, the normalized difference vegetation index (NDVI) and enhanced vegetation index (EVI) reflect comparable rice-growth curves to the AVHRR LAI. Therefore,

they can be used as an ancillary remote sensing product to retrieve crop phenology at regions where the AVHRR LAI are absent and vice versa.

In addition to covering a larger spatiotemporal scale, the rice calendars obtained in this study showed comparable or even better accuracy than previous studies. For example, RMSE between the retrieved and referenced phenology ranged from 17 to 44 days in a study by You et al. [34], which was much greater than the RMSE range in this study (9–14 days). The R^2 between the retrieved and referenced phenology was greater than 0.90 in a study by Luo et al. [13], and so was the accuracy of the transplanting and harvesting dates in this study. As for the lengths of different growing stages, most of our results were identical to the published USDA and RiceAtlas data, although a few countries had slightly longer periods based on the retrieved phenology, such as the Republic of Korea and Japan. After generating the creditable retrieved phenology, we further revealed more spatial characteristics on the decadal changes of rice calendars (Figure 5). The ground observation changes could validate our remote-sensing-retrieved calendar changes in some countries. For example, Zhang et al. [4] analyzed phenology data from agrometeorological stations and also found that the lengths of most growing stages were prolonged for the late season in China. To our knowledge, more spatial characteristics in this study were first indicated for some Southeast Asian countries (i.e., Cambodia), which would greatly enrich researchers' understanding of rice-cropping-system development.

4.2. Improvements in Identifying Climate Contributions on Rice Calendar Changes

Through regressing the six most general climatic variables with rice calendars for main cropping seasons, our study filled the gap of the Asia-wide investigation on how multiple climatic variables impact rice calendars. Climate change is the biggest natural factor on crop calendars. Many studies have investigated how a single climatic variable impacts crop phenology, either in a specific country or at the regional scale. For example, rising temperatures shortened the GP for early rice, prolonged the GP for late rice, and had less impact on the GP for single rice in China [35–37]. Chen et al. [38] incorporated temperature, precipitation, and sunshine hours into a linear regression model to estimate the phenology response in China. He found that the maximum positive sensitivity came from the sunshine hour and the maximum negative sensitivity was from temperature. However, Asia-wide monitoring of rice phenology requires more comprehensive analysis for all rice-cropping areas. To the best of our knowledge, this study is the first to compare the effects of different climatic variables across the main rice-cropping seasons in Asia. Our results highlighted that *srad* had the greatest impact on rice calendars, followed by t_{max} and t_{min}. These findings were almost identical to those of Chen et al. [38]. Rice-cropping areas at lower latitudes are more vulnerable to climate change, and the most sensitive period was the VGP. Therefore, tropical areas during the VGP should be monitoring hotspots in food security systems.

4.3. Uncertainties and Limitations

This study, like many others, also had some uncertainties.

First, we applied the two most classical methods, the threshold-based and inflection-based methods, to retrieve phenological dates from the GLASS AVHRR LAI (8-day repeat cycle at $0.05^\circ \times 0.05^\circ$ scale). However, considering main rice seasons always rotate with other crops or another short-termed rice in Asia, threshold-based and inflection-based methods might fail to identify the precise phenology from the irregular LAI curves [39]. Thus, developing novel methods aimed at improving calendar accuracy is a worthwhile focus of future research [40]. Furthermore, we used the GLASS AVHRR LAI from 1995–2015 with the aim of obtaining a long-time series of remote sensing data, but its spatial resolution was moderate. Therefore, the mixed-pixel problems affected the accuracy of the retrieved phenological dates. Other general remote sensing products with a finer spatial resolution always have a coarser temporal resolution or a shorter period. For example, all Landsat data are in a 16-day repeat cycle at 30 m; Landsat 5 TM data starts at 1984 but ends in 2012 [41,42].

We anticipate that long-term remote sensing products with high spatial–temporal resolution will be available in the near future.

Second, crop phenology is mainly affected by natural and anthropogenic factors [1,4]. To separate the effects of climate factors on rice calendar changes, we used the first-difference regression method to eliminate the long-term impact of the improved technology. However, in addition to climate variables and technologies, other factors, such as soil type and local farmers' fieldwork, might influence the spatial variance of rice calendar changes. The properties of one specific type of soil, such as soil temperature, soil water content, and soil nutrition, could elicit earlier or later crop phenology [43–45]. Site-specific experiments provide possible ways to explore the mechanisms of the crop calendar responses to local soil changes and further support relevant solutions to adjust crop growth. In addition, large-scale ground surveys of farmers' fieldwork (such as fertilizer and irrigation) could enrich researchers' understanding of anthropogenic contributions [46,47]. Nevertheless, many studies indicated that crop cultivars played the dominant role in crop growth [1,4,35], which might be of great use in adapting crop growth to natural and anthropogenic surrounding changes.

Last but not the least, there are uncertainties related to the referenced data in this study. The limited availability of annually referenced calendars in most countries meant that we had to calculate the averages of retrieved phenological dates from 1995–2015 before comparing them with the retrieved and referenced phenology in Figure 3. Similarly, the midpoint of mid-season in the USDA was used as the observed heading dates because of the lack of referenced heading information. Therefore, it is vitally important to develop ground-monitoring systems to facilitate long-term field observations, which will not only enable remote sensing phenology detections but also benefit other agricultural studies aimed at sustaining food security.

5. Conclusions

Identifying rice calendar changes is vitally important in Asia, where rice plays a dominant role in farmers' livelihoods, but cropping systems are complex. Through generating grid-scale key phenological dates from the GLASS AVHRR LAI for 17 main rice-cropping seasons in Asia, we identified the spatiotemporal characteristics of the rice calendar changes and their climate drivers. The overall accuracy of the retrieved phenological dates was comparable to the ground observations. The VGP is the most vulnerable growing period because it has the greatest length changes and sensitivity to climate change, especially in tropical areas. Compared with previous studies focusing on specific countries or limited periods, our study provides new findings covering a greater spatiotemporal range, which will assist governments and researchers regarding the development of agricultural policies aimed at maintaining national food security.

Author Contributions: Conceptualization, J.Z. and H.W.; methodology, J.Z.; software, J.Z.; validation, H.W. and L.Z.; formal analysis, J.Z.; investigation, H.W., L.Z. and Y.L.; data curation, Y.L. and J.H.; writing—original draft preparation, J.Z.; writing—review and editing, Z.Z.; visualization, J.Z.; supervision, Z.Z. and F.T.; funding acquisition, J.Z., Z.Z. and F.T. All authors have read and agreed to the published version of the manuscript.

Funding: This research was funded by the National Key Research and Development Project of China (2020YFA0608201), China National Postdoctoral Program for Innovative Talents (BX20200064), and National Natural Science Foundation of China (42061144003, 41977405, 42101095).

Data Availability Statement: Data are available on request from the authors.

Conflicts of Interest: The authors declare no conflict of interest.

References

1. Piao, S.; Liu, Q.; Chen, A.; Janssens, I.A.; Fu, Y.; Dai, J.; Liu, L.; Lian, X.U.; Shen, M.; Zhu, X. Plant phenology and global climate change: Current progresses and challenges. *Glob. Chang. Biol.* **2019**, *25*, 1922–1940. [CrossRef] [PubMed]
2. Ettinger, A.K.; Chamberlain, C.J.; Morales-Castilla, I.; Buonaiuto, D.M.; Flynn, D.F.B.; Savas, T.; Samaha, J.A.; Wolkovich, E.M. Winter temperatures predominate in spring phenological responses to warming. *Nat. Clim. Chang.* **2020**, *10*, 1137–1142. [CrossRef]
3. Kawatsu, S.; Homma, K.; Horie, T.; Shiraiwa, T. Change of weather condition and its effect on rice production during the past 40 years in Japan. *Jpn. J. Crop. Sci.* **2007**, *76*, 423–432. [CrossRef]
4. Zhang, L.; Zhang, Z.; Zhang, J.; Luo, Y.; Tao, F. Response of rice phenology to climate warming weakened across China during 1981–2018: Did climatic or anthropogenic factors play a role? *Environ. Res. Lett.* **2022**, *17*, 064029. [CrossRef]
5. Bandumula, N. Rice production in Asia: Key to global food security. *Proc. Natl. Acad. Sci. India Sect. B Biol. Sci.* **2018**, *88*, 1323–1328. [CrossRef]
6. Laborte, A.G.; Gutierrez, M.A.; Balanza, J.G.; Saito, K.; Zwart, S.J.; Boschetti, M.; Murty, M.V.R.; Villano, L.; Aunario, J.K.; Reinke, R.; et al. RiceAtlas, a spatial database of global rice calendars and production. *Sci. Data* **2017**, *4*, 1–10. [CrossRef]
7. Mishra, B.; Busetto, L.; Boschetti, M.; Laborte, A.; Nelson, A. RICA: A rice crop calendar for Asia based on MODIS multi year data. *Int. J. Appl. Earth Obs. Geoinf.* **2021**, *103*, 102471. [CrossRef]
8. Wang, C.; Zhang, Z.; Chen, Y.; Tao, F.; Zhang, J.; Zhang, W. Comparing different smoothing methods to detect double-cropping rice phenology based on LAI products—A case study in the Hunan province of China. *Int. J. Remote Sens.* **2018**, *39*, 6405–6428. [CrossRef]
9. Zhang, J.; Zhang, Z.; Wang, C.; Tao, F. Double-rice system simulation in a topographically diverse region—A remote-sensing-driven case study in Hunan Province of China. *Remote Sens.* **2019**, *11*, 1577. [CrossRef]
10. Zhang, X.; Friedl, M.A.; Schaaf, C.B.; Strahler, A.H.; Hodges, J.C.; Gao, F.; Reed, B.C.; Huete, A. Monitoring vegetation phenology using MODIS. *Remote Sens. Environ.* **2003**, *84*, 471–475. [CrossRef]
11. Boschetti, M.; Stroppiana, D.; Brivio, P.A.; Bocchi, S. Multi-year monitoring of rice crop phenology through time series analysis of MODIS images. *Int. J. Remote Sens.* **2009**, *30*, 4643–4662. [CrossRef]
12. Boschetti, M.; Busetto, L.; Manfron, G.; Laborte, A.; Asilo, S.; Pazhanivelan, S.; Nelson, A. PhenoRice: A method for automatic extraction of spatio-temporal information on rice crops using satellite data time series. *Remote Sens. Environ.* **2017**, *194*, 347–365. [CrossRef]
13. Luo, Y.; Zhang, Z.; Chen, Y.; Li, Z.; Tao, F. ChinaCropPhen1km: A high-resolution crop phenological dataset for three staple crops in China during 2000–2015 based on leaf area index (LAI) products. *Earth Syst. Sci. Data* **2020**, *12*, 197–214. [CrossRef]
14. Thackeray, S.J.; Henrys, P.A.; Hemming, D.; Bell, J.R.; Botham, M.S.; Burthe, S.; Helaouet, P.; Johns, D.G.; Jones, I.D.; Leech, D.I.; et al. Phenological sensitivity to climate across taxa and trophic levels. *Nature* **2016**, *535*, 241–245. [CrossRef]
15. Yang, L.H.; Rudolf, V. Phenology, ontogeny and the effects of climate change on the timing of species interactions. *Ecol. Lett.* **2010**, *13*, 1–10. [CrossRef]
16. Fu, Y.H.; Zhao, H.; Piao, S.; Peaucelle, M.; Peng, S.; Zhou, G.; Ciais, P.; Huang, M.; Menzel, A.; Peñuelas, J.; et al. Declining global warming effects on the phenology of spring leaf unfolding. *Nature* **2015**, *526*, 104–107. [CrossRef]
17. Han, J.; Zhang, Z.; Luo, Y.; Cao, J.; Zhang, L.; Zhuang, H.; Cheng, F.; Zhang, J.; Tao, F. Annual paddy rice planting area and cropping intensity datasets and their dynamics in the Asian monsoon region from 2000 to 2020. *Agric. Syst.* **2022**, *200*, 103437. [CrossRef]
18. Xiao, Z.; Liang, S.; Wang, J.; Chen, P.; Yin, X.; Zhang, L.; Song, J. Use of general regression neural networks for generating the GLASS leaf area index product from time-series MODIS surface reflectance. *IEEE Trans. Geosci. Remote Sens.* **2013**, *52*, 209–223. [CrossRef]
19. Xiao, Z.; Liang, S.; Wang, J.; Xiang, Y.; Zhao, X.; Song, J. Long-time-series global land surface satellite leaf area index product derived from MODIS and AVHRR surface reflectance. *IEEE Trans. Geosci. Remote Sens.* **2016**, *54*, 5301–5318. [CrossRef]
20. Claverie, M.; Matthews, J.L.; Vermote, E.F.; Justice, C.O. A 30+ year AVHRR LAI and FAPAR climate data record: Algorithm description and validation. *Remote Sens.* **2016**, *8*, 263. [CrossRef]
21. Zhu, Z.; Bi, J.; Pan, Y.; Ganguly, S.; Anav, A.; Xu, L.; Samanta, A.; Piao, S.; Nemani, R.R.; Myneni, R.B. Global data sets of vegetation Leaf Area Index (LAI)3g and Fraction of Photosynthetically Active Radiation (FPAR)3g derived from Global Inventory Modeling and Mapping Studies (GIMMS) Normalized Difference Vegetation Index (NDVI3g) for the period 1981 to 2011. *Remote Sens.* **2013**, *5*, 927–948.
22. Liu, Y.; Liu, R.; Chen, J.M. Retrospective retrieval of long-term consistent global leaf area index (1981–2011) from combined AVHRR and MODIS data. *J. Geophys. Res.—Biogeosci.* **2012**, *117*, G04003. [CrossRef]
23. Xiao, Z.; Liang, S.; Jiang, B. Evaluation of four long time-series global leaf area index products. *Agric. For. Meteorol.* **2017**, *246*, 218–230. [CrossRef]
24. Gao, X.; Liang, S.; He, B. Detected global agricultural greening from satellite data. *Agric. For. Meteorol.* **2019**, *276*, 107652. [CrossRef]
25. Kumar, S.V.; Mocko, D.M.; Wang, S.; Peters-Lidard, C.D.; Borak, J. Assimilation of remotely sensed leaf area index into the Noah-MP land surface model: Impacts on water and carbon fluxes and states over the continental United States. *J. Hydrometeorol.* **2019**, *20*, 1359–1377. [CrossRef]

26. Zhao, Y.; Feng, J.; Luo, L.; Bai, L.; Wan, H.; Ren, H. Monitoring Cropping Intensity Dynamics across the North China Plain from 1982 to 2018 Using GLASS LAI Products. *Remote Sens.* **2021**, *13*, 3911. [CrossRef]
27. Abatzoglou, J.T.; Dobrowski, S.Z.; Parks, S.A.; Hegewisch, K.C. TerraClimate, a high-resolution global dataset of monthly climate and climatic water balance from 1958–2015. *Sci. Data.* **2018**, *5*, 1–12. [CrossRef]
28. Chen, Y.; Zhang, Z.; Tao, F.; Palosuo, T.; Rötter, R.P. Impacts of heat stress on leaf area index and growth duration of winter wheat in the North China Plain. *Field Crops Res.* **2018**, *222*, 230–237. [CrossRef]
29. Sakamoto, T.; Yokozawa, M.; Toritani, H.; Shibayama, M.; Ishitsuka, N.; Ohno, H. A crop phenology detection method using time-series MODIS data. *Remote Sens. Environ.* **2005**, *96*, 366–374. [CrossRef]
30. Sakamoto, T.; Van Nguyen, N.; Ohno, H.; Ishitsuka, N.; Yokozawa, M. Spatio–temporal distribution of rice phenology and cropping systems in the Mekong Delta with special reference to the seasonal water flow of the Mekong and Bassac rivers. *Remote Sens. Environ.* **2006**, *100*, 1–16. [CrossRef]
31. Liu, Y.; Zhou, W.; Ge, Q. Spatiotemporal changes of rice phenology in China under climate change from 1981 to 2010. *Clim. Chang.* **2019**, *157*, 261–277. [CrossRef]
32. Pan, B.; Zheng, Y.; Shen, R.; Ye, T.; Zhao, W.; Dong, J.; Ma, H.; Yuan, W. High resolution distribution dataset of double-season paddy rice in China. *Remote Sens.* **2021**, *13*, 4609. [CrossRef]
33. Soh, N.C.; Shah, R.M.; Giap, S.G.E.; Setiawan, B.I.; Minasny, B. High-Resolution Mapping of Paddy Rice Extent and Growth Stages across Peninsular Malaysia Using a Fusion of Sentinel-1 and 2 Time Series Data in Google Earth Engine. *Remote Sens.* **2022**, *14*, 1875.
34. You, X.; Meng, J.; Zhang, M.; Dong, T. Remote sensing based detection of crop phenology for agricultural zones in China using a new threshold method. *Remote Sens.* **2013**, *5*, 3190–3211. [CrossRef]
35. Tao, F.; Zhang, Z.; Shi, W.; Liu, Y.; Xiao, D.; Zhang, S.; Zhu, Z.; Wang, M.; Liu, F. Single rice growth period was prolonged by cultivars shifts, but yield was damaged by climate change during 1981–2009 in China, and late rice was just opposite. *Glob. Chang. Biol.* **2013**, *19*, 3200–3209. [CrossRef]
36. Hu, X.; Huang, Y.; Sun, W.; Yu, L. Shifts in cultivar and planting date have regulated rice growth duration under climate warming in China since the early 1980s. *Agric. For. Meteorol.* **2017**, *247*, 34–41. [CrossRef]
37. Ye, T.; Zong, S.; Kleidon, A.; Yuan, W.; Wang, Y.; Shi, P. Impacts of climate warming, cultivar shifts, and phenological dates on rice growth period length in China after correction for seasonal shift effects. *Clim. Chang.* **2019**, *155*, 127–143. [CrossRef]
38. Chen, J.; Liu, Y.; Zhou, W.; Zhang, J.; Pan, T. Effects of climate change and crop management on changes in rice phenology in China from 1981 to 2010. *J. Sci. Food Agric.* **2021**, *101*, 6311–6319. [CrossRef]
39. Manfron, G.; Delmotte, S.; Busetto, L.; Hossard, L.; Ranghetti, L.; Brivio, P.A.; Boschetti, M. Estimating inter-annual variability in winter wheat sowing dates from satellite time series in Camargue, France. *Int. J. Appl. Earth Obs.* **2017**, *57*, 190–201. [CrossRef]
40. Gao, F.; Zhang, X. Mapping crop phenology in near real-time using satellite remote sensing: Challenges and opportunities. *J. Remote Sens.* **2021**, *2021*, 8379391. [CrossRef]
41. Hansen, M.C.; Loveland, T.R. A review of large area monitoring of land cover change using Landsat data. *Remote Sens. Environ.* **2012**, *122*, 66–74. [CrossRef]
42. Claverie, M.; Vermote, E.F.; Franch, B.; Masek, J.G. Evaluation of the Landsat-5 TM and Landsat-7 ETM+ surface reflectance products. *Remote Sens. Environ.* **2015**, *169*, 390–403. [CrossRef]
43. Estiarte, M.; Peñuelas, J. Alteration of the phenology of leaf senescence and fall in winter deciduous species by climate change: Effects on nutrient proficiency. *Glob. Chang. Biol.* **2015**, *21*, 1005–1017. [CrossRef] [PubMed]
44. Stone, P.J.; Sorensen, I.B.; Jamieson, P.D. Effect of soil temperature on phenology, canopy development, biomass and yield of maize in a cool-temperate climate. *Field Crops Res.* **1999**, *63*, 169–178. [CrossRef]
45. Ata-Ul-Karim, S.T.; Cang, L.; Wang, Y.; Zhou, D. Effects of soil properties, nitrogen application, plant phenology, and their interactions on plant uptake of cadmium in wheat. *J. Hazard. Mater.* **2020**, *384*, 121452. [CrossRef]
46. Li, C.; Tang, Y.; Luo, H.; Di, B.; Zhang, L. Local farmers' perceptions of climate change and local adaptive strategies: A case study from the Middle Yarlung Zangbo River Valley, Tibet, China. *Environ. Manag.* **2013**, *52*, 894–906. [CrossRef]
47. Liu, Y.; Zhang, J.; Pan, T.; Ge, Q. Assessing the adaptability of maize phenology to climate change: The role of anthropogenic-management practices. *J. Environ. Manag.* **2021**, *293*, 112874. [CrossRef]